Construction of WO$_3$ coatings with micro-nano hybrid structures by liquid precursor flame spray for enhanced sensing performances to sub-ppm ozone

Jing Huang [a], Xiaoxia Wang [b], Yongfeng Gong [a], Yi Liu [a], Ping Zhou [a], Xinkun Suo [a], Dawei Zeng [b], Hua Li [a,*]

[a] Key Laboratory of Marine Materials and Related Technologies, Zhejiang Key Laboratory of Marine Materials and Protective Technologies, Ningbo Institute of Materials Technology and Engineering, Chinese Academy of Sciences, Ningbo 315201, China
[b] State Key Laboratory of Materials and Processing Die & Mould Technology, Huazhong University of Science and Technology, Wuhan 430074, China

ARTICLE INFO

ABSTRACT

WO$_3$ coatings with tunable micro-nano hybrid structures were fabricated by liquid precursor flame spraying. The coatings consisting of the sole component of monoclinic WO$_3$ show porous topographical morphology with grains of ~20 nm and pores of ~4–8 μm. Assessment of gas sensing performances of the coatings to ozone reveals their optimum operating temperature of 150 °C, and sensor response of 3.9 and 46.7 to ozone concentration of 0.5 ppm and 2.0 ppm respectively. The results shed light on construction of ceramic coatings with tunable hybrid structures by the precursor flame spray technical route for functional applications.

© 2017 Elsevier B.V. All rights reserved.

1. Introduction

Ozone (O$_3$) is almost everywhere as a result of the interaction between sunlight and certain chemicals emitted into the environment [1]. As a strong oxidizing agent, when the concentration of ozone exceeds a certain threshold value, its exposure becomes hazardous to human health, causing serious health problems [2]. Therefore, detecting and monitoring ozone or its mixtures is of critical importance and is indispensable [3]. Among the sensors developed nowadays, solid-state sensors are attractive owing to their unique advantages [4,5]. A variety of metal-oxide semiconductors have recently been attempted for ozone detection [6]. Previous studies have shown that WO$_3$ is an ideal ozone-sensing material, and has the advantages of high sensitivity, quick response time and sensing compatibility particularly to ozone [6,7]. Many methods have been tried for making WO$_3$ coatings/films, such as sol–gel, thermal evaporation, hydrothermal, chemical vapor deposition, and thermal spray [8,9]. Liquid thermal spray processing offers simplicity of operation, capability of spraying nano-structured materials and controllable construction of coating microstructure [8,10]. It is established that microstructural charac-teristics of the coatings/films play crucial roles in deciding their long-term sensitivity and selectivity of targeted gas. Gas sensors require a porous microstructure with small particle size to supply large specific surface area [10]. Fabrication of novel WO$_3$ coatings with desired structures for promoted sensing performances however remains challenging.

In this work, liquid precursor flame spray (LPFS) processing route was proposed aiming to fabricate WO$_3$ coatings with micro-nano hybrid structures for enhanced ozone sensing performances with significantly reduced optimum operating temperature. Microstructural features and ozone-sensing properties of the coatings were characterized and elucidated. The LPFS approach might open a new window for making nano-ceramics films for functional applications.

2. Materials and methods

Commercial alumina plates equipped with Au electrodes and Pt heat element were used as the substrate for WO$_3$ coating deposition. WCl$_6$ (Aladdin Reagent Corp., China) was used for pyrolysis synthesis of WO$_3$ by flame spraying and polyethylene glycol (PEG, Sino Pharm, China) was used as surfactant. For the spraying, PEG was dissolved in deionized water and WCl$_6$ was dissolved in anhydrous ethyl alcohol. After ultrasonic cleaning for 20 min, the
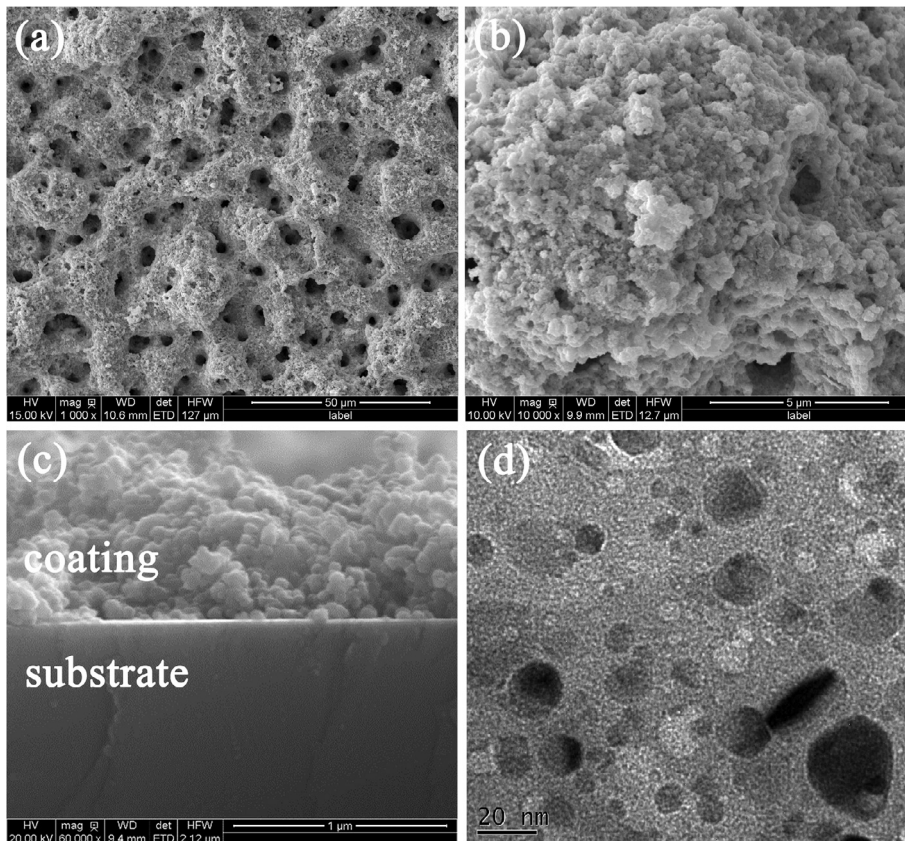
Fig. 1. SEM images showing the topographical (a, b) and cross-sectional (c) microstructure of the WO_3 coating, and (d) TEM image showing the spherical nanosized WO_3 grains.
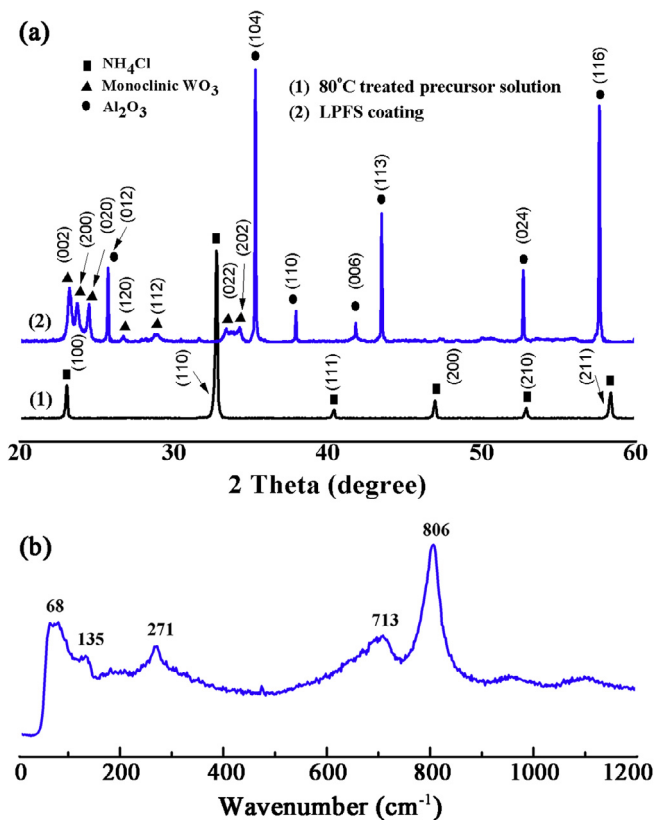

Fig. 2. XRD patterns (a) and Raman spectrum (b) of the coatings.

dissolved WCl_6 was mixed with the PEG solution under constant magnetic stirring. pH value of the mixture was stabilized at 7–8 as adjusted by ammonium hydroxide solution. During the spraying, the liquid precursor feedstock was atomized by a spray gun operated using the compressed air of 0.7 MPa. The precursor feedstock injector of 1.5 mm in diameter was positioned next to flame torch, and the angle between the injector and flame was 30°. The CDS-8000 flame spray system (Eutectic Castolin, UK) was employed for the coating deposition. The pressure and flow rate of oxygen was 0.5 MPa and 2.5 Nm^3/hr, respectively. Acetylene was used as combustion gas with a pressure of 0.1 MPa and flow rate of 1.5 Nm^3/hr. The spray distance was 15 cm and the liquid precursor feeding rate was 40 ml/min.

Chemistry of the coatings was examined by Raman spectrometry (Renishaw inVia Reflex, UK) and X-ray diffraction (XRD, PANalytical X'pert Pro, the Netherlands) using Cu Kα radiation operated at 35 mA and 40 kV. Microstructure of the coatings was characterized using field emission scanning electron microscopy (FESEM, FEI Quanta FEG250, the Netherlands) and transmission electron microscopy (TEM, FEI Tecnai F20, the Netherlands). Sensing performances of the coatings to ozone were measured in a Teflon chamber. Ozone gas was generated by a FL-8F ozone generator (Feili Ltd., China) and the gas with the concentrations of 0.5–10.0 ppm was calibrated by an ozone detector (HJ-BXA-O₃, Huijin Ltd., China). Heat treatment at 200 °C for 24 h in ambient air was conducted for the coatings prior to the gas-sensing testing, and each sensing measurement was replicated three times. Sensor response or sensitivity (S) was defined as $S = R_{ozone}/R_{air}$, where R_{ozone} and R_{air} are the electric resistance of the sensor device exposed to ozone and dry air, respectively [11].

Table 1
Comparison of the sensor response versus T_{opt} and O_3 concentration.

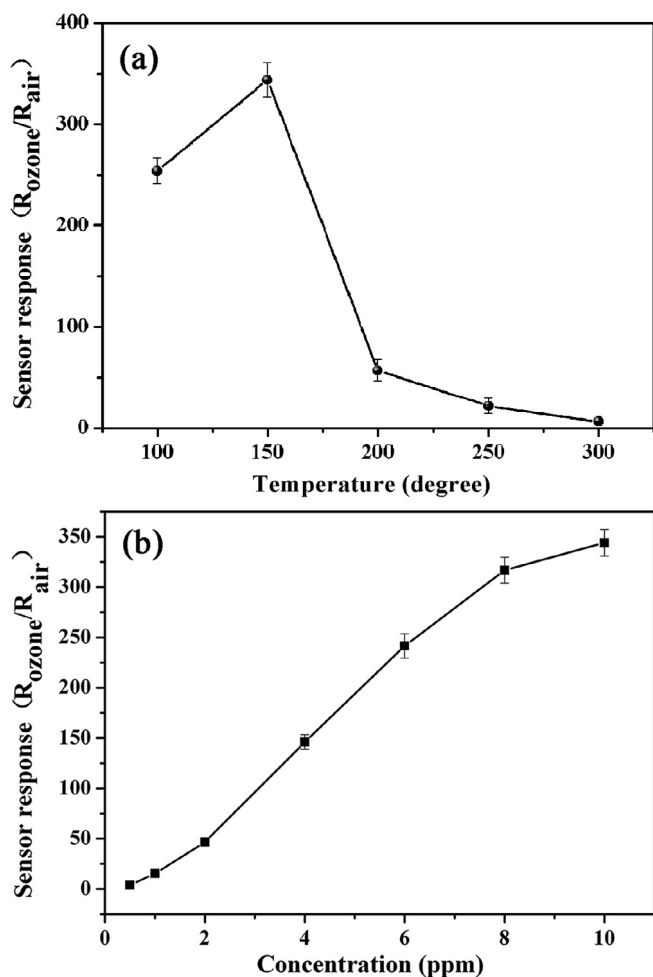| Sensors	Method	T_{opt}/°C	O_3 /ppm	Response /S	Refs.
Nano-ZnO	Hydrothermal method	250	1.2	9	[12]
$Zn_2In_2O_5$-$MgIn_2O_4$	RF sputtering	275	0.4, 5	1, 10	[14]
WO_3	RF sputtering	250	0.8	2.8	[16]
Nano-WO_3	LPFS	150	0.5	3.9	This study
			1.0	15.3	
			2.0	46.7	

Fig. 3. Gas sensing performances of the coatings, (a) sensor response to 10 ppm O_3 measured at various working temperatures, and (b) sensor response versus ozone concentration.

3. Results and discussion

Microstructural characterization of the coatings suggests that the nano-WO_3 particles tend to aggregate into submicron-sized clusters during coating formation stage and interconnecting particles form micro-porous structure with the pore size of ∼4–8 µm (Fig. 1a and b). Moreover, the submicron-sized aggregates are accumulated by spherical nanosized grains of ∼20 nm and the coating thickness of ∼700 nm has been achieved (Fig. 1c and d). Many parameters play important roles in influencing the structural features of the coatings, such as pH value, anhydrous ethyl alcohol content, and PEG content of the precursor solution, and flow rate of oxygen, acetylene pressure, and spray distance for the flame spray. Among the parameters, pH value, anhydrous ethyl alcohol, and concentration of PEG of the precursor solution were found to be

the key parameters deciding construction of the micro-nano hybrid structures. Compared to the porous structural characteristics, the thickness of the coatings plays minor role in regulating their sensing performances. This is predominately because adsorption/desorption of gases is directly related to features of the exposed structures of the coatings on their top surfaces. The micro-nano hybrid porous structure gives rise to large specific surface area, which would facilitate ozone gas adsorption and multiply reaction sites for ozone-WO_3 reaction [4].

Further phase analysis reveals predominate presence of monoclinic WO_3 in the coatings (Fig. 2). Since the coatings are very thin, the peaks for alumina substrate are also detected. To clarify the stage at which crystalline WO_3 forms during the spraying, the starting precursor suspension was dried at 80 °C for 10 h for following XRD analyses. The dried powder shows the presence of NH_4Cl, while no trace of WO_3 is seen (Fig. 2a), indicating that monoclinic WO_3 is synthesized during the spraying. The chemical reaction of WCl_6 with RCH_2OH usually yields HCl and $(RCH_2O)_mWCl_n$, and $(RCH_2O)_mWCl_n$ takes part in etherification reaction to form WO_3 by capturing water molecules [8]. The chemistry of the coatings was further characterized by Raman spectroscopy (Fig. 2b). The phonon bands at 806 cm^{-1} and 713 cm^{-1} are assigned to the O-W-O stretching mode and the peak at 806 cm^{-1} refers to the vibration of shorter bonds. The W-O-W bending mode of bridging oxygen is located at 271 cm^{-1}, and the peak at 135 cm^{-1} is assigned to lattice vibrations of WO_3 [12]. Those peaks are typical ones for monoclinic WO_3.

To determine the optimum operating temperature (T_{opt}), the WO_3 coating sensor was exposed to 10 ppm ozone and the measurement was made at different temperatures ranging from 100 °C to 300 °C. Results show that there is a systematic increase in response with increased operating temperature below 150 °C. Reverse tendency is observed above 150 °C. This phenomenon has also been observed by other researchers for different sensor materials [11,13]. Compared to the T_{opt} of WO_3 coatings fabricated by traditional methods and of other traditional metal oxide ozone sensors [11,14,16], much lower T_{opt} with higher sensor response at low concentration ozone condition is achieved in this work (Table 1).

The sensor made from the nanostructured WO_3 was then kept at 150 °C with the exposure to different O_3 levels. It is realized that the sensor response gets significantly increased from 3.9 to 346.3 when the ozone concentration increases (Fig. 3b). The porous WO_3 coating with micro-nano hybrid structure shows exciting sensitivity to ozone at the concentrations of sub-ppm levels.

The sensing mechanism of n-type semiconductor sensors has been well elucidated by the surface-depletion model [17]. As a typical n-type sensor material, upon exposure to air, WO_3 would interact with oxygen by transferring electrons from conductance band to adsorbed oxygen atoms, forming ionic species, such as O_2^-, O^-, and O^{2-} [7,14]. At room temperature, oxygen ions exist mainly in the form of O_2^-. When oxygen partial pressure or temperature changes, O_2^- may decompose to O_2 and release e^- [13–15]. In this case, O_3 is adsorbed onto WO_3 surface, extracting electrons from the conduction band of WO_3 and in turn reducing the number of

charge carriers. Consequently, the barrier of WO₃ is increased, and the resistance of the WO₃ coating is increased whenever O₃ is adsorbed onto WO₃ surface [7,15]. Compared with the structures in micron-sized scale, the micro-nano microstructure of the porous WO₃ coating shows excellent ozone sensitivity. This is presumably owing to the fact that the porous microstructure provides more gas adsorption and reaction sites which usually speed up the reaction between metal oxide and adsorbed gas [8].

4. Conclusions

Porous WO₃ coatings with micro-nano hybrid microstructures have been successfully fabricated by liquid precursor flame spraying. The micro-nano porous WO₃ sensor exhibits exciting ozone sensitivity and response time at 150 °C, and has good sensitivity to ozone at sub-ppm concentration levels. The results would give insight into cost-effective fabrication of functional ceramic coatings by liquid precursor flame spray route for versatile applications.

Acknowledgments

References

[1] Z. Zhu, J.L. Chang, R.J. Wu, Sens. Actuators B: Chem. 214 (2015) 56.
[2] L.S.R. Rocha, C.R. Foschini, C.C. Silva, E. Longo, A.Z. Simoes, Ceram. Int. 42 (2016) 4539.
[3] L.F. da Silva, A.C. Catto, W. Avansi, L.S. Cavalcante, J. Andres, K. Aguir, V.R. Mastelaro, E. Longo, Nanoscale 6 (2014) 4058.
[4] Y. Park, K.Y. Dong, J. Lee, J. Choi, G.N. Bae, B.K. Ju, Sens. Actuators B: Chem. 140 (2009) 407.
[5] A. Labidi, C. Jacolin, M. Bendahan, A. Abdelghani, J. Guerin, K. Aguir, M. Maaref, Sens. Actuators B: Chem. 106 (2005) 713.
[6] G. Korotcenkov, Handbook of gas sensor materials: properties, Advantages and Shortcomings for Applications, Springer, New York, 2013.
[7] M. Suchea, N. Katsarakis, S. Christoulakis, M. Katharakis, T. Kitsopoulos, G. Kiriakidis, Anal. Chim. Acta 573–574 (2006) 9.
[8] Q.F. Wu, J. Huang, H. Li, Mater. Lett. 141 (2015) 100.
[9] G.F. Fine, L.M. Cavanagh, A. Afonja, R. Binions, Sensors 10 (2010) 5469.
[10] G. Biasotto, M.G.A. Ranieri, C.R. Foschini, A.Z. Simoes, E. Longo, M.A. Zaghete, Ceram. Int. 40 (2014) 14991.
[11] A.C. Catto, L.F. da Silva, C. Ribeiro, S. Bernardini, K. Aguir, E. Longo, V.R. Mastelaro, RSC Adv. 5 (2015) 19528.
[12] T. Siciliano, A. Tepore, G. Micocci, A. Serra, D. Manno, E. Filippo, Sens. Actuators B: Chem. 133 (2008) 321.
[13] L.F. da Silva, V.R. Mastelaro, A.C. Catto, C.A. Escanhoela, S. Bernardini, S.C. Zilio, E. Longo, K. Aguir, J. Alloy Compd. 638 (2015) 374.
[14] T. Miyata, T. Hikosaka, T. Minami, Surf. Coat. Technol. 126 (2000) 219.
[15] C. Zhang, M. Debliquy, A. Boudiba, H. Liao, C. Coddet, Sens. Actuators B: Chem. 144 (2010) 280.
[16] S. Vallejos, V. Khatko, J. Calderer, I. Gracia, C. Cane, E. Llobet, X. Correig, Sens. Actuators B: Chem. 132 (2008) 209.
[17] N. Barsan, U.D.O. Weimar, J. Electroceram. 7 (2002) 143.